ELSEVIER

Infrared Physics & Technology 42 (2001) 177–184

INFRARED PHYSICS & TECHNOLOGY

www.elsevier.com/locate/infrared

A detailed study of non-uniform quantum well infrared photodetectors

S.Y. Wang [a,*], Y.C. Chin [b], C.P. Lee [b]

[a] *Institute of Astronomy and Astrophysics, Academia Sinica, Nankang, Taipei 11592, Taiwan, ROC*

[b] *Department of Electronic Engineering, National Chiao Tung University, 1001 Ta-Hsueh Road, Hsinchu 30050, Taiwan, ROC*

Abstract

A non-uniform quantum well infrared photodetector (NUQWIP) structure is studied. By changing the doping concentration and barrier width of each quantum well, the electric field distribution can be tailored. Different transition types of NUQWIPs were fabricated. Suppressed dark current is obtained for all the NUQWIPs. The NUQWIPs show excellent performance compared with conventional uniform structures. The dark current is about an order of magnitude lower and the background limited temperature increases for 6°. The electric field distribution within the structure is calculated to explain the results and characteristics of the NUQWIPs. The NUQWIP is found to be advantageous for the low cutoff energy detectors using B–C transitions. © 2001 Published by Elsevier Science B.V.

PACS: 85.60.Gz; 73.50.Pz

Keywords: Quantum well; Intersubband; Infrared detector

1. Introduction

In the past decade, a great deal of effort has been put into the development of quantum well infrared photodetectors (QWIPs) [1]. The promising performance made QWIPs a good competitor to traditional HgCdTe detectors. However, despite all the advantages of QWIPs, they usually suffer from high dark current. So one is usually forced to operate the QWIPs below 77 K in order to meet the readout circuit requirement and to achieve the background limited operation. In a conventional QWIP structure, the same quantum well and barriers are repeated 30–50 times. The optimization of the QWIP structure is usually concerned with the design of the quantum wells and the barriers but not the structure as a whole. However, some recent studies have revealed that the quantum wells cannot be treated the same [2–4]. The depletion of the first few wells was found, and it is the cause of the power non-linearity of the responsivity at high voltages [4]. So, it is clear that the electric field distribution can greatly change the QWIPs' characteristics.

Recently, we purposely used a non-uniform quantum well structure in a QWIP to alter the distribution of the electric field [5]. The doping concentration and the barrier width is not the same for all the quantum wells in the new structure. Lower dark currents and higher gains were obtained with the non-uniform QWIPs (NUQWIPs).

* Corresponding author.

1350-4495/01/$ - see front matter © 2001 Published by Elsevier Science B.V.
PII: S1350-4495(01)00074-3

The BLIP temperature is increased by 6° compared to that of the conventional QWIPs. In this work, more detailed properties of NUQWIPs are investigated using samples with different transition types and different non-uniform designs. Besides, the temperature dependence of responsivity is also measured and discussed.

2. Experiments

Samples used in this work were grown by MBE on (1 0 0) semi-insulating GaAs substrates. Three different sets of samples were made using bound to continuum (B–C set 1), bound to quasi bound (B–QB set 2), and bound to bound (B–B set 3) transitions. Each set consisted of one conventional QWIP and one NUQWIP. Detailed quantum well parameters are listed in Table 1. In set 1, 35 quantum wells were used for the active region while for set 2 and 3, 30 quantum wells were used. For the non-uniform structure, as the growth progressed, the barrier width was decreased from 850 to 150 Å, while the doping concentration in the well was increased from 5×10^{16} to 4×10^{18} cm^{-3}. The distributions of the doping concentration in the wells and the barrier width are shown in Fig. 1. Most of the doping concentration change was made in the first few wells and the barrier width changes almost linearly. The width of all the quantum wells was kept the same. The Si dopants in each well were put in the center 25 Å region. The upper and bottom contact layers were 0.8 μm n-type GaAs with a doping concentration of 2×10^{18} cm^{-3}. For comparison, a standard sample with a uniform quantum well structure was also prepared. The barrier height and the well width were kept the same as the non-uniform structure to ensure the same absorption spectrum. The barrier width and the doping concentration of all the quantum wells were 500 Å and 5×10^{17} cm^{-3}, respectively. The total sheet doping concentration and the barrier width were designed to be the same for both structures, so the absorbance of the samples was kept at the same value. The changes made in the non-uniform structure were to adjust the electric field distribution in the device. After the layers were grown, the absorption spectra were measured by a FTIR using a 45° waveguide configuration. Almost the same absorption characteristics were obtained for both samples in each set. After that, 200 μm square mesas were defined and formed by chemical etching. Au/Ge was put on the top and the bottom of the mesas for ohmic contacts. Finally, a 45° facet is polished at the wafer edge for the following optical measurement.

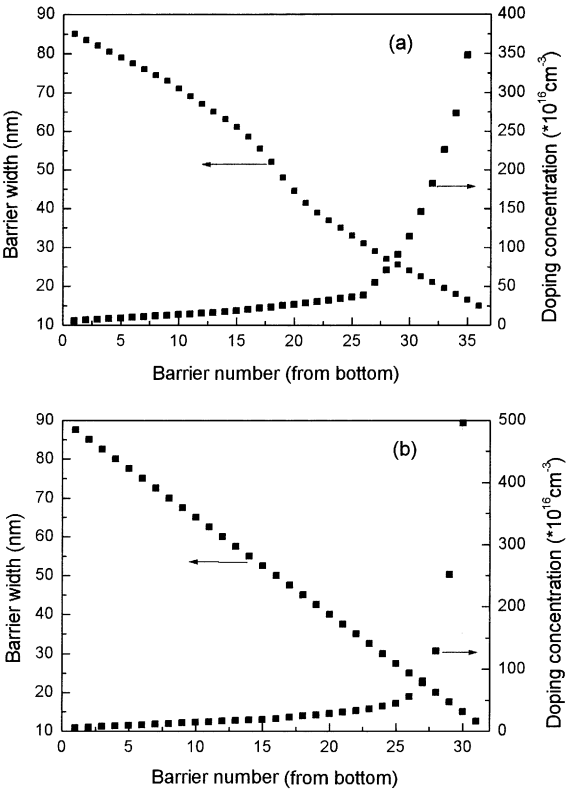

Fig. 1. The distributions of doping concentration and barrier width of each quantum wells for the NUQWIP in (a) sample set 1 and (b) sample set 2 and 3.

Table 1
The structure parameters of the three sample sets

Sample set	Well width (Å)	Barrier Al content	Periods	Average doping (10^{17} cm^{-3})
1 (B–C)	45	24	35	5
2 (B–QB)	45	27	30	5
3 (B–B)	55	29	30	5

3. Results and discussion

After the devices were fabricated, dark current–voltage (I–V) characteristics at different temperatures and the 300 K background photocurrent at 10 K were measured using a close cycled helium cryostat. In all the measurements, the bottom contact is referenced as ground. The photoresponses of the devices were measured at different temperatures by a FTIR spectrometer, and calibrated by a 1000 K blackbody source.

3.1. Basic characteristics of NUQWIP and B–C NUQWIPs

Fig. 2 shows the I–V characteristics of sample set 1, the dark current of the NUQWIP at 77 K is about an order of magnitude lower than that of the conventional structure. But the 300 K background photocurrent is almost the same and even larger. Because of the lower dark current, the BLIP temperature (with a field of view of 40°) of the new NUQWIP is significantly increased for about 6 degree to 67 K, compared to the conventional uniform QWIP prepared side by side.

To understand why the dark current of the NUQWIPs is lower, we need to know the electric field distribution in the devices. Using the concept of current continuity and balancing the number of carriers trapped by and the number of carriers escaped from each quantum well, the electric field distribution can be calculated [3]. Fig. 3(a) shows the calculated potential profiles of the NUQWIP under forward and reverse biases. For comparison, the potential distribution of a conventional structure is shown in Fig. 3(b). Because of the non-uniform doping and barrier width, the electric field in the NUQWIP is quite non-uniform. In the highly doped region, the number of free carriers is high so the electric field is low. On the other hand, the lowly doped region has a high electric field.

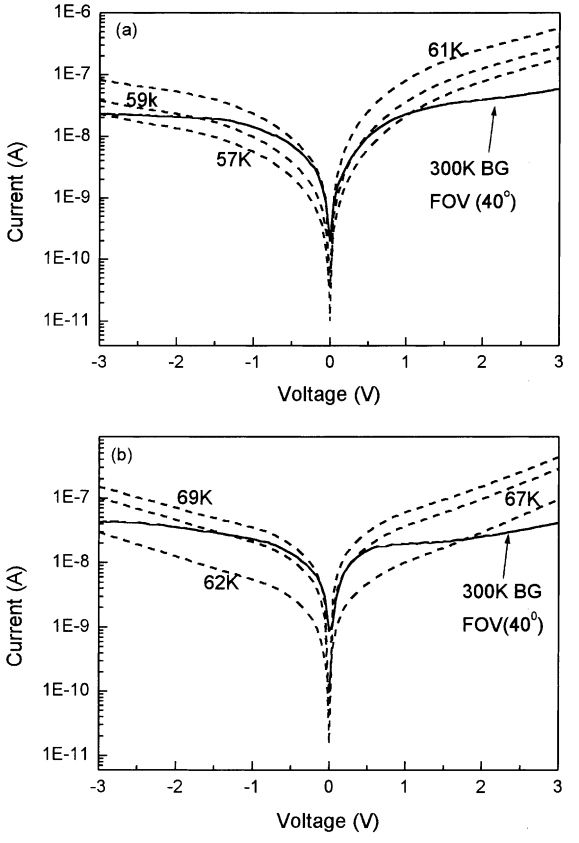

Fig. 2. The dark current at different temperatures and the 300 K background photocurrent for (a) a conventional QWIP and (b) a NUQWIP in sample set 1.

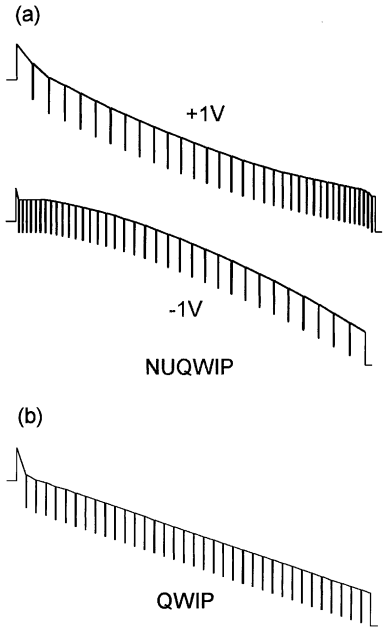

Fig. 3. The calculated voltage distribution of (a) a NUQWIP under ±1 V and (b) a conventional QWIP at 1 V.

This highly non-uniform field distribution gives the possibility to reduce the dark current. Due to the large dynamic resistance of the low doping wells, the dark current is limited over large value of electric field and only very small electric field can fall on the high doping wells. The long barriers of the low doping wells increase the bias taken by these wells and this further lower the voltage drop at high doping region. The doping concentration of the wells that under high electric field (higher than the average electric field) is lower than half of the concentration used in the conventional sample. Therefore, we can see that the dark current of a conventional structure is higher than that of a non-uniform structure if they have the same total sheet carrier density. This is true for both forward and reverse bias conditions.

The responsivity spectrum and the bias dependence of the response are shown in Fig. 4. The peak responsivity is at 9.7 μm with $\Delta\lambda/\lambda = 20\%$. Although the dark current of this device is much lower, we found that the responsivity at reverse bias is still very good and is larger than that of the uniform structure. In the NUQWIPs, the high doping wells are close to the cathode in the reverse bias case and in this region the electric field is very small. So the electron's escape probability is small and the resulting quantum efficiency of these quantum wells also suffers. For the rest of the structure, since the average doping concentration is lower than that of the quantum wells in the uniform structure, the quantum efficiency is lower. Therefore the overall quantum efficiency of the non-uniform structure should be lower than that of the uniform structure. The reason that we measured very good responsivity for the new structure is due to the increased gain in the device.

We have measured the noise spectral density of the devices. From the obtained noise i_n and the dark current I_d, the gain can be calculated using the following relationship (assuming that the *G–R* noise dominates):

$$g_n = \frac{i_n}{4qI_d}$$

The bias dependence of the noise gain for both samples at reverse bias is shown in Fig. 5. For the NUQWIP, the gain increases with bias and saturates at a value of 3 at reverse bias. For the conventional QWIP, the gain saturates at about 0.5. The increased gain in the NUQWIP can also be understood from the electric field distribution in the device. As shown in Fig. 2, at a reverse bias of

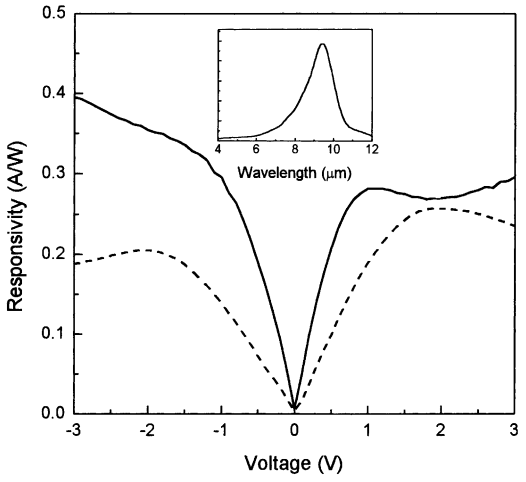

Fig. 4. The voltage dependence of responsivity of the sample set 1. The solid line represents the responsivity of NUQWIP and the dashed line shows the responsivity of the conventional QWIP. The insert shows the responsivity spectrum of the NUQWIP.

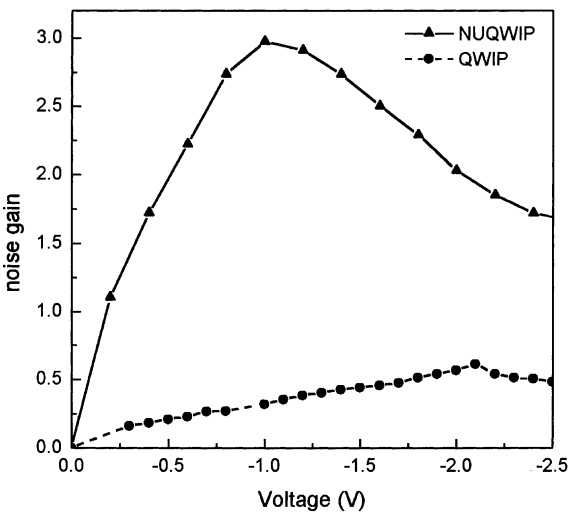

Fig. 5. The noise gain vs. voltage plot for the sample set 1 under reverse bias.

1.0 V, the electric field in the first few barriers (near the cathode) is nearly zero and then the electric field increases. Near the anode, the electric field becomes very large and is larger than 14 kV/cm. This strong field can induce impact ionization. The electrons, which gain enough energy from the field, can interact with the confined electrons inside the quantum well to excite the carriers out of the well. This effect has been found in QWIPs at large biases [6]. The threshold energy to induce impact ionization is about the same as the activation energy for the carriers in the quantum well and can be even lower if tunneling is taken into consideration [7]. For the quantum well structure that we use, the activation energy is about 110 meV. In the region close to the anode, the barriers are quite thick (The last one is 850 Å). If we take the thickness of those barriers to be 800 Å, the electric field needed to induce ionization is about 13.5 kV/cm. Thus, the impact ionization happens in this region at -1 V. Under this situation, we have to reexamine the gain that we found from noise. The noise spectral density with the presence of impact ionization is

$$i_n = 4qgi_d\,\Delta f\left[M^2\left(2-\frac{1}{M}\right)\right]$$

where M is the multiplication factor and g is the gain without multiplication. If we assume there is no impact ionization for the uniform QWIP (at least for voltages not too high), we can use the g value of the uniform QWIP in the above equation. If we take g to be 0.5, which is the saturated gain of the uniform QWIP, we obtain a multiplication factor of 2 at -1 V for the NUQWIP using the above equation. For conventional QWIPs, the electric field is much more uniform. Under the same bias voltage, the electric field is around 7 kV/cm, which is well below the threshold needed for impact ionization. When the NUQWIP is forward biased, the maximum electric field is also lower than that when it is reverse biased. That is why the saturated gain is lower in the forward direction. So in NUQWIPs, even when the quantum efficiency is lower than that of the conventional structure, the responsivity is still good because of a higher gain. At higher biases, the multiplication factor continues to increase and the electron escape probability for higher doping wells also increases, so the responsivity can increase without saturation. Combining the noise and the responsivity results, the detectivity of the devices at 77 K is calculated. For the NUQWIP, the detectivity is 7.5×10^9 cm $\mathrm{Hz}^{1/2}$/W at -1 V and maintains the same value to about -2.5 V. But for the conventional structure, the detectivity is 3.5×10^9 cm $\mathrm{Hz}^{1/2}$/W at -1 V and decreases to 2.5×10^9 cm $\mathrm{Hz}^{1/2}$/W at -1.5 V.

3.2. Other transition types of NUQWIPs

From the discussion above, we know that the advantages of NUQWIP comes from the nonuniform electric field distribution and the resulting impact ionization multiplication. The multiplication process directly relates to the cutoff energy and the excited state energy. Fig. 6 shows the I–V characteristics of sample set 2. As expected, the dark current of NUQWIP is again lower than the conventional one. The BLIP temperature also increases for 4 to about 74 K. However, the responsivity of the NUQWIPs is lower than the conventional one as shown in Fig. 7. The B–QB samples have a peak responsivity at 8.4 μm with $\Delta\lambda/\lambda = 11\%$. The responsivity of NUQWIPs increases faster with voltage but becomes smaller than that of the conventional one. The larger slope of the responsivity curve indicates the large field in the low doping region. The large field can give higher escape probability of the excited electrons and thus enhance the responsivity. The change of cutoff energy and excited state energy can explain the decrease of the responsivity of the NUQWIP. Comparing to the B–C sample, the B–QB sample has a lower excited state energy which decreases the escape probability in the high doping region where the field is always small [8]. The total quantum efficiency is therefore lower compared to that of the sample with the B–C transition. The cutoff energy increases by about 20 meV for the B–QB sample. The higher cutoff energy requires a larger electric field for impact multiplication. Combining these two effects, the responsivity for the NUQWIP is lower than the conventional one. However, because of a lower dark current, the performance is still better than the conventional

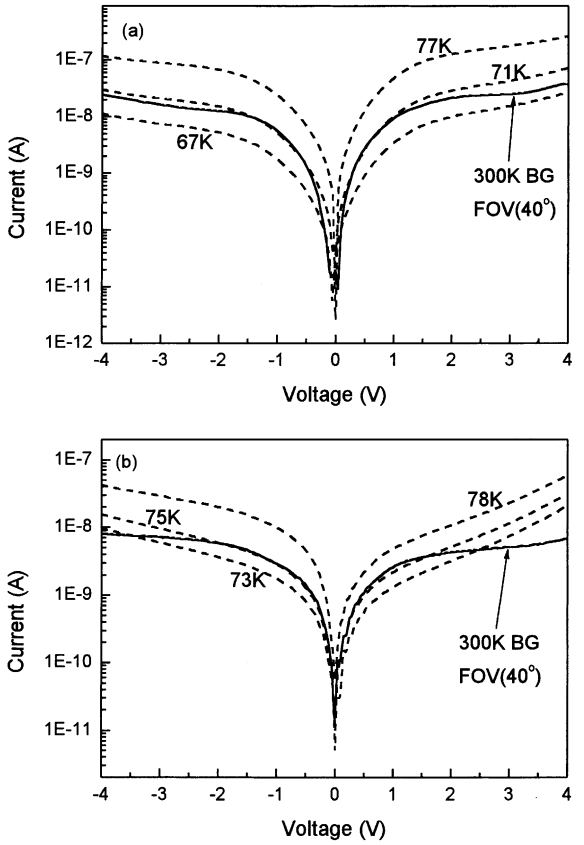

Fig. 6. The dark current at different temperatures and the 300 K background photocurrent for (a) a conventional QWIP and (b) a NUQWIP in sample set 2.

QWIP. The detectivity (3×10^{10} cm $Hz^{1/2}$/W at -2 V) is about 1.5 times that of the conventional sample.

For sample set 3, more confined excited state further decreases the escape probability. The quantum efficiency for the high doping wells is nearly zero. This decreases the total quantum efficiency and responsivity a lot. Fig. 8 shows the responsivity curves and the spectra of these samples. The B–B samples have peak responsivity at 9.0 μm with $\Delta\lambda/\lambda = 8\%$. At low biases, the high field in the low doping region decreases the onset voltage of the responsivity curve. But, after the conventional one turns on, the responsivity is about 1.5 of that of the NUQWIPs. Although the dark current is still lower for the NUQWIP, the BLIP temperature is the same as the conventional

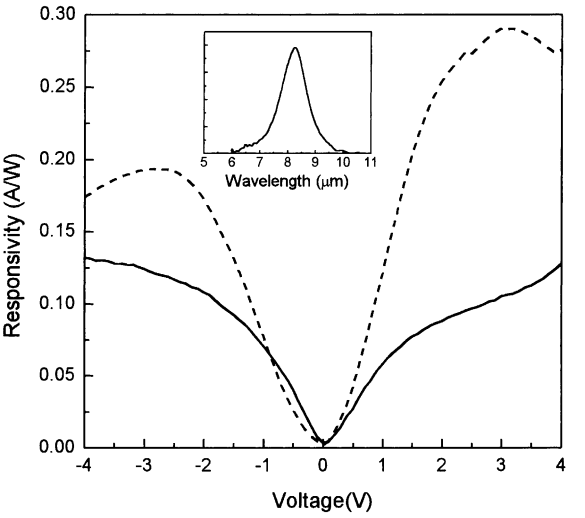

Fig. 7. The voltage dependence of responsivity of the sample set 2. The solid line represents the responsivity of NUQWIP and the dashed line shows the responsivity of the conventional QWIP. The insert shows the responsivity spectrum of the NUQWIP.

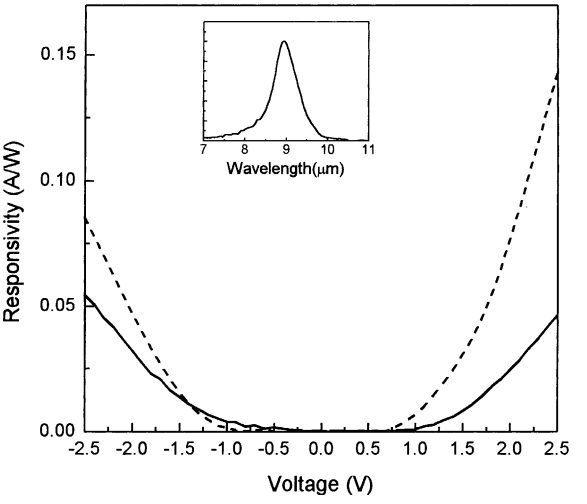

Fig. 8. The voltage dependence of responsivity of the sample set 3. The solid line represents the responsivity of NUQWIP and the dashed line shows the responsivity of the conventional QWIP. The insert shows the responsivity spectrum of the NUQWIP.

one (68 K). The detectivity is also the same as the conventional one which is about 1.0×10^{10} cm $Hz^{1/2}$/W.

3.3. Temperature dependence of NUQWIPs

For conventional QWIPs, the responsivity remains the same as the temperature changes. The uniform electric field distribution is maintained over the long quantum well region lat different temperatures. The temperature dependent responsivity was only found in the QWIPs with a single QW. However, the change of temperature changes the injection current out of each QW. For NUQWIPs, different temperature dependence of each QW changes the electric field distribution through the QWs and the responsivity changes. Fig. 9 shows the responsivity curve at different temperatures. The responsivity is almost the same under reverse bias but increases with temperature under forward bias. The corresponding voltage distribution is calculated and shown in Fig. 10. Due to the lower injection current of the low doping wells, the electric field distribution separates into two parts at low temperatures. An uniform high field domain exists and leaves a long almost zero field region. The responsivity is thus lower due to the low quantum efficiency and high capture probability in this region. As the temperature increases, this low field region decreases and the responsivity increase gradually.

In additional to the samples mentioned above, samples with different doping and barrier distributions were also fabricated. The distribution can be altered by different designs. For example, a linear distribution of doping can create a uniform build-in electric field that can produce a photovoltaic device. Low dark current devices can be made by wells with large difference in doping concentration. The way to suppress the dark current is to increase the electric field in the low doping region and to decrease the possibility of high electric field in the high doping region. The high doping region can provide a higher quantum efficiency which is a necessity for high responsivity.

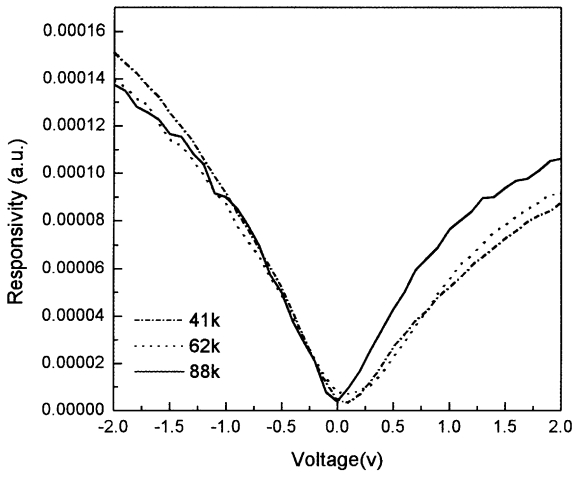

Fig. 9. The voltage dependence of responsivity of the B–QB NUQWIP at different temperatures.

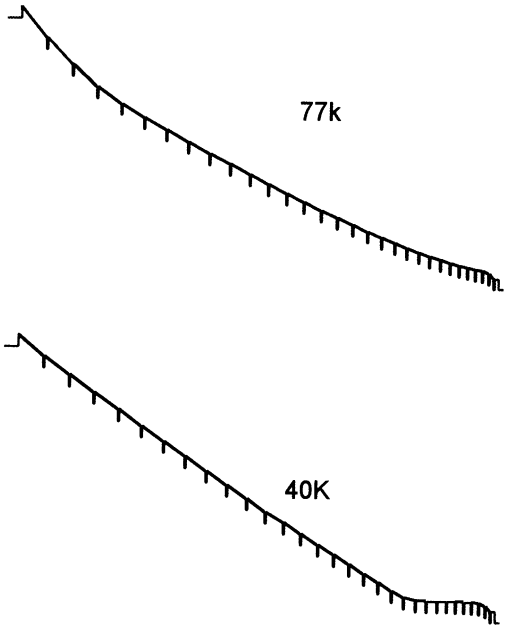

Fig. 10. The calculated voltage distribution of the B–QB NUQWIP at 77 and 40 K at 1 V.

4. Conclusion

In conclusion, a NUQWIP structure is described. By changing the doping concentration and barrier width of each well, the electric field distribution can be changed. The change in the electric field has a great influence on the detector's performance. The dark current can always be lower as long as the non-uniform doping distribution is used. The NUQWIP is found to be most effective

for the bound to continuum type detectors. The impact ionization and the gain are significantly higher than those of the conventional uniform structure. Both the detectivity and the BLIP temperature are increased for the NUQWIPs. For a 9.2 μm cutoff B–QB device, the detectivity can be as high as 3×10^{10} cm $Hz^{1/2}$/W with a 74 K BLIP temperature (FOV 40°) using 45° coupling. The dark current density is only 2×10^{-5} cm^{-2}. The use of the NUQWIP in the very long wavelength is expected to be of great potential.

Acknowledgements

The authors would like to thank Professor C.H. Kuan and M.C. Hsu of National Taiwan University for the noise measurements. This work is supported by the National Science Council under Contract No. NSC89-2215-E009-013.

References

[1] B.F. Levine, J. Appl. Phys. 74 (1993) R1–R81.
[2] M. Ershov, V. Ryzhii, C. Hamaguchi, Appl. Phys. Lett. 67 (1995) 3147–3149.
[3] L. Thibaudeau, P. Bois, J.Y. Duboz, J. Appl. Phys. 79 (1996) 446–454.
[4] A. Sa'ar, C. Mermelstein, H. Schneider, C. Schoenbein, M. Walther, in: S.S. Li, Y.K. Su (Eds.), Intrersubband Transitions in Quantum Wells: Physics and Devices, Kluwer Academic, Dordrecht, 1998, pp. 60–67.
[5] S.Y. Wang, C.P. Lee, J. Appl. Phys. 87 (2000) 522–525.
[6] B.F. Levine, K.K. Choi, C.G. Bethea, J. Walker, R.J. Malik, Appl. Phys. Lett. 51 (1987) 934–936.
[7] S.L. Chuang, K. Hess, J. Appl. Phys. 59 (1986) 2885–2894.
[8] B.F. Levine, A. Zussman, S.D. Gunapala, M.T. Asom, J.M. Kuo, W.S. Hobson, J. Appl. Phys. 72 (1992) 4429–4443.